Supplement of

Analysis of atmospheric CH_4 in Canadian Arctic and estimation of the regional CH_4 fluxes

Misa Ishizawa et al.

Correspondence to: Misa Ishizawa (misa.ishizawa@canada.ca)

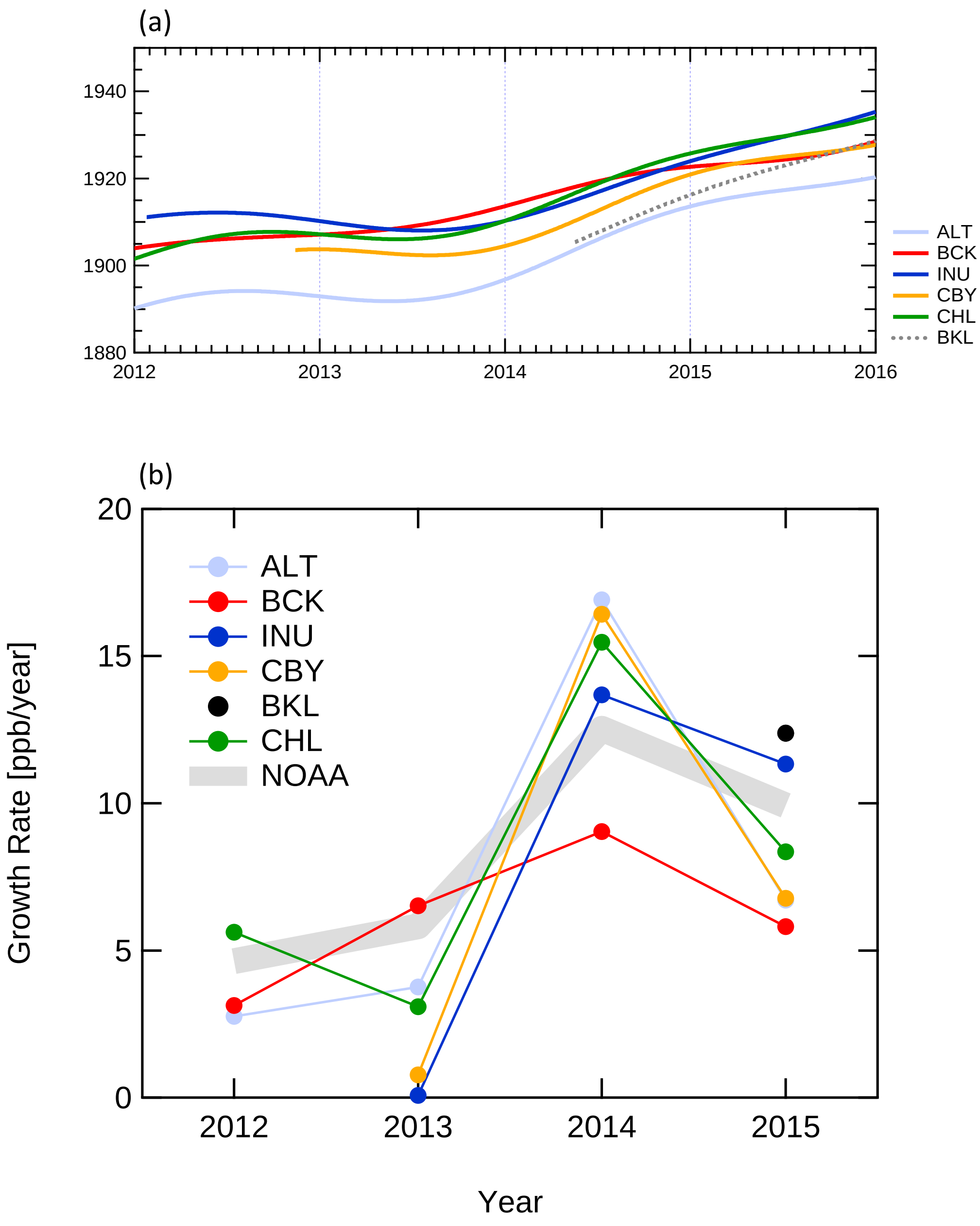

Figure S1: Growth rates of atmospheric CH_4 observed at Canadian Arctic sites. For comparison, NOAA annual increase from globally-averaged atmospheric CH_4 is plotted. The growth rates of Canadian Arctic sites are obtained in the similar manner with NOAA annual increase. The growth rate is defined by the difference in CH_4 concentration on January 1st from January 1st of the previous year in the long-term trend curves (shown in Fig. 2, seasonal components are removed).

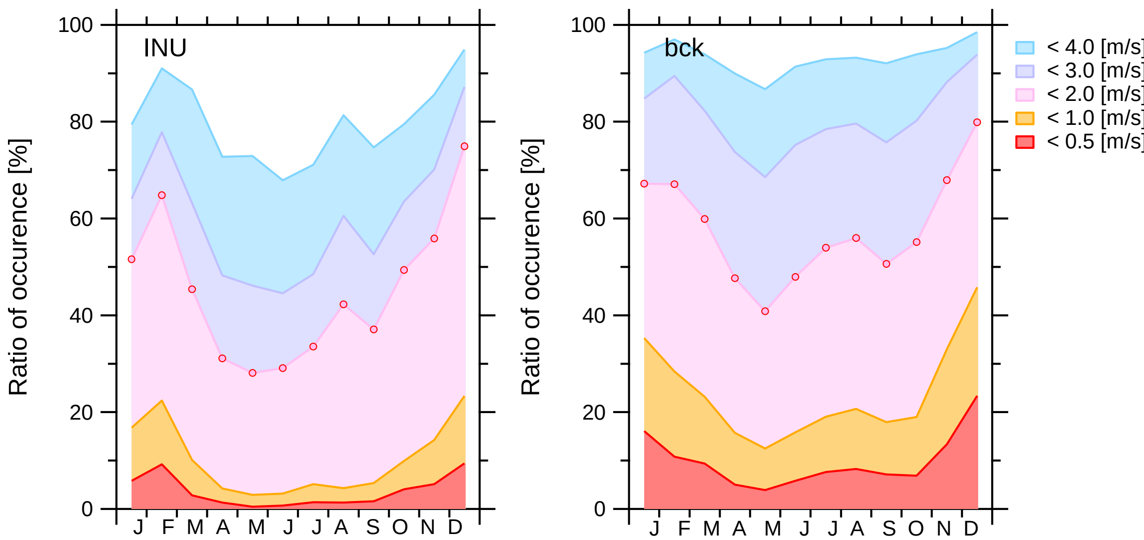

Figure S2: Mean seasonal cycles of wind speed at Inuvik (INU) and Behchoko (BCK). At INU, the hourly wind data are obtained at the Inuvik ECCC upper air weather station where the GHG measurement system is situated. At BCK, the wind speed has been measured independently of the ECCC weather network. The wind speed data for 2012-2015 are grouped by wind speed and normalized per month.

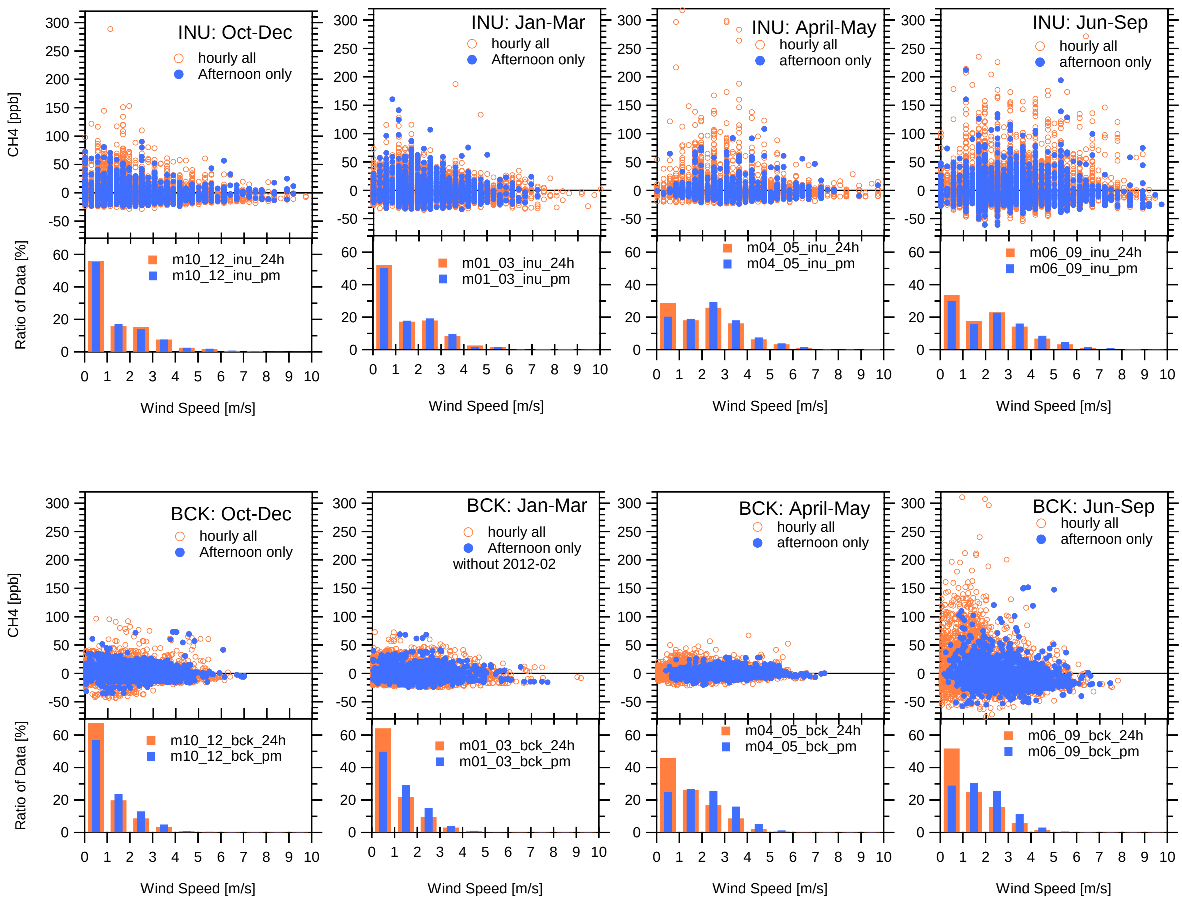

Figure S3: Variability of observed hourly CH_4 concentrations at Inuvik (INU) and Behchoko (BCK). The variability is defined as the deviations of observed CH_4 from the fitted curves (shown in Fig. 2).

Mask A (3 sub-regions)

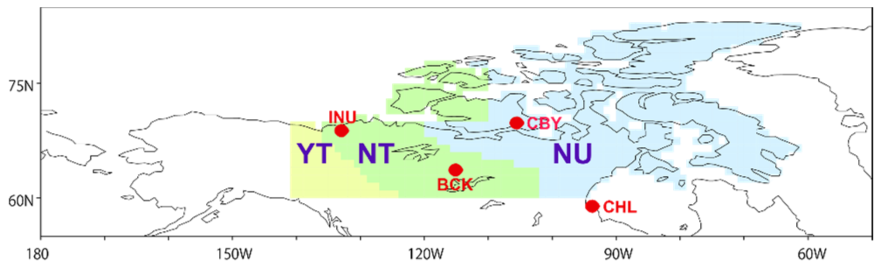

Mask B (2 sub-region)

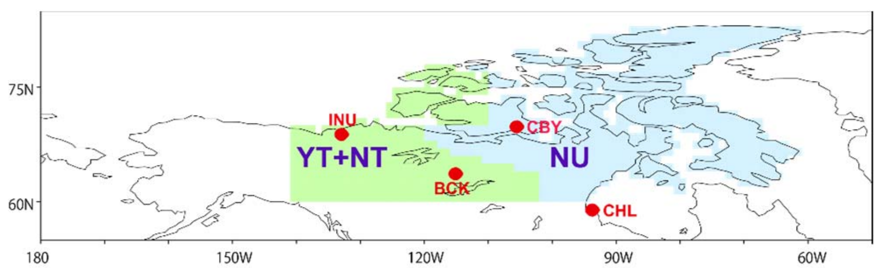

Mask C

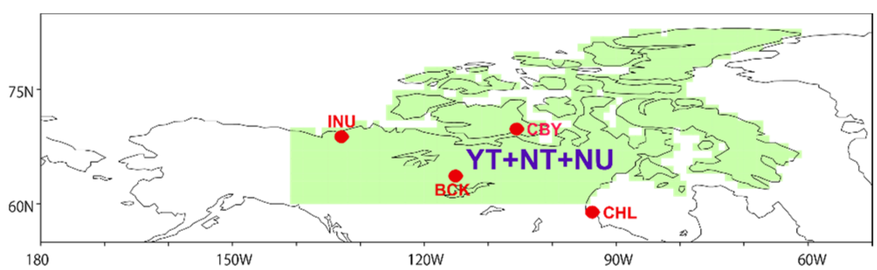

Figure S4: Sub-regions used for the regional inversion. Initially, the Canadian Arctic is sub-divided based on territory boundaries. Mask A: three regions of YT (Yukon), NT (Northwest Territories) and NU (Nunavut), Mask B: Two regions by combining NT and YT, and Mask C: one region as combining all territories YT, NT and NU. The four continuous measurement sites used for the inversion are plotted in the red closed circles.

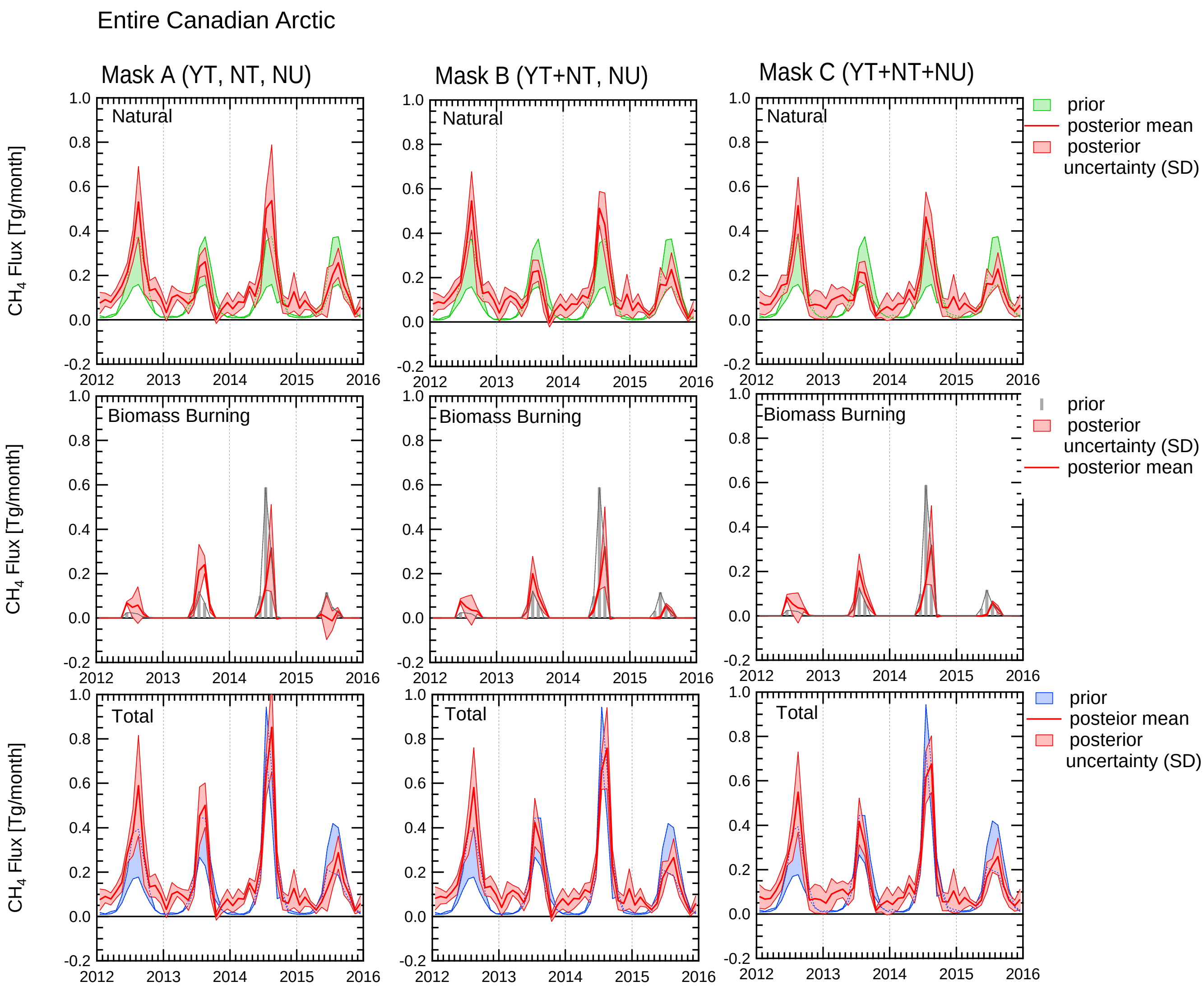

Figure S5: Monthly posterior fluxes, same with Fig. 8, but for the entire Canadian Arctic with three different sub-region masks. The sub-regional fluxes with Mask A and Mask B are aggregated.

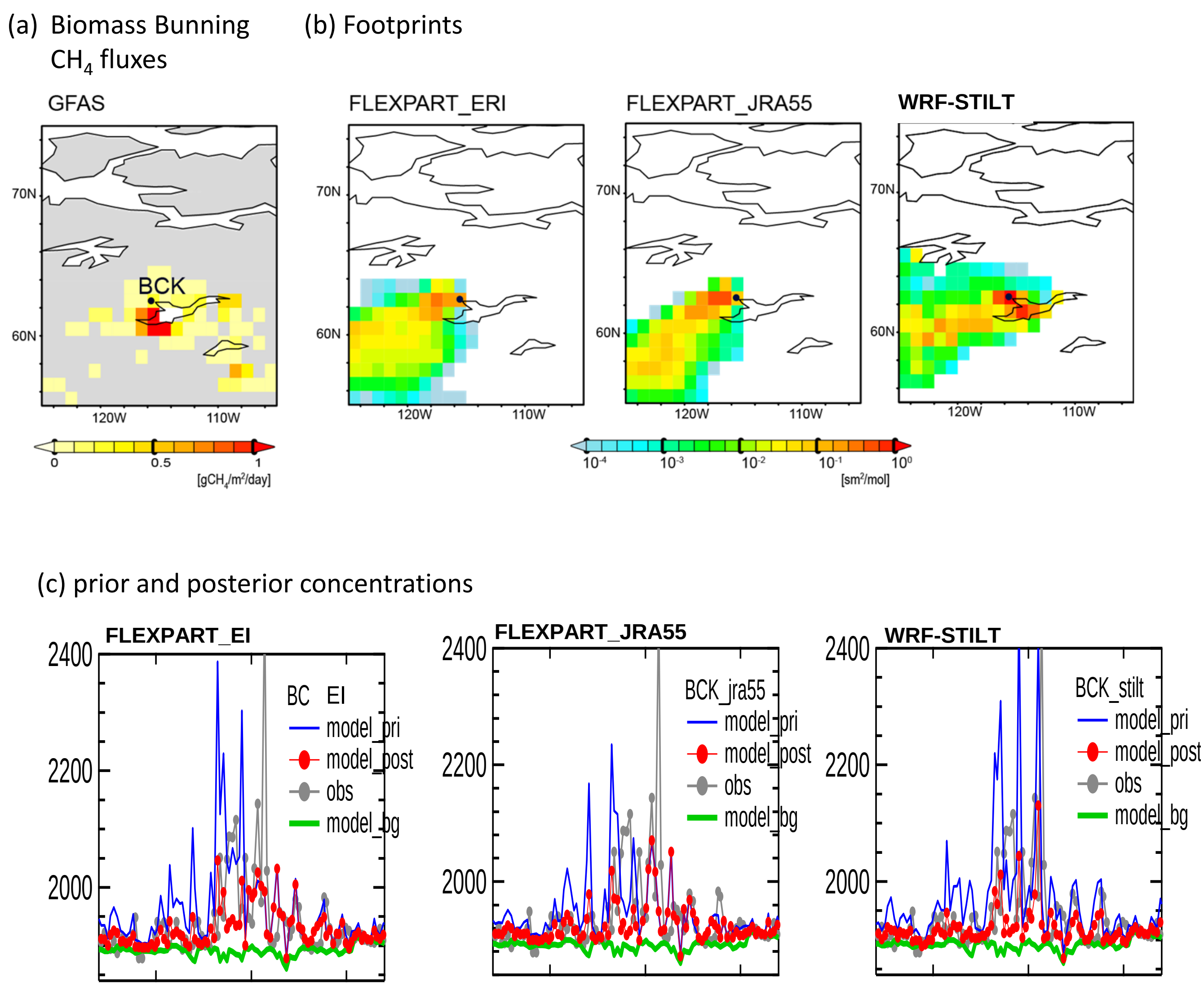

Figure S6: **(a) Prior biomass burning CH_4 emissions from GFAS for August 5, 2014. (b) 5-day back trajectory footprints of BCK for August 5, 2014, by FLEXPART_EI, FLEXPART_JRA55 and WRF-STILT. (c) prior (blue) and posterior (red) concentrations at BCK for the summer in 2014 with Mask B and prior flux case C3. Observations (gray) and modelled background concentrations (green) are also plotted.**

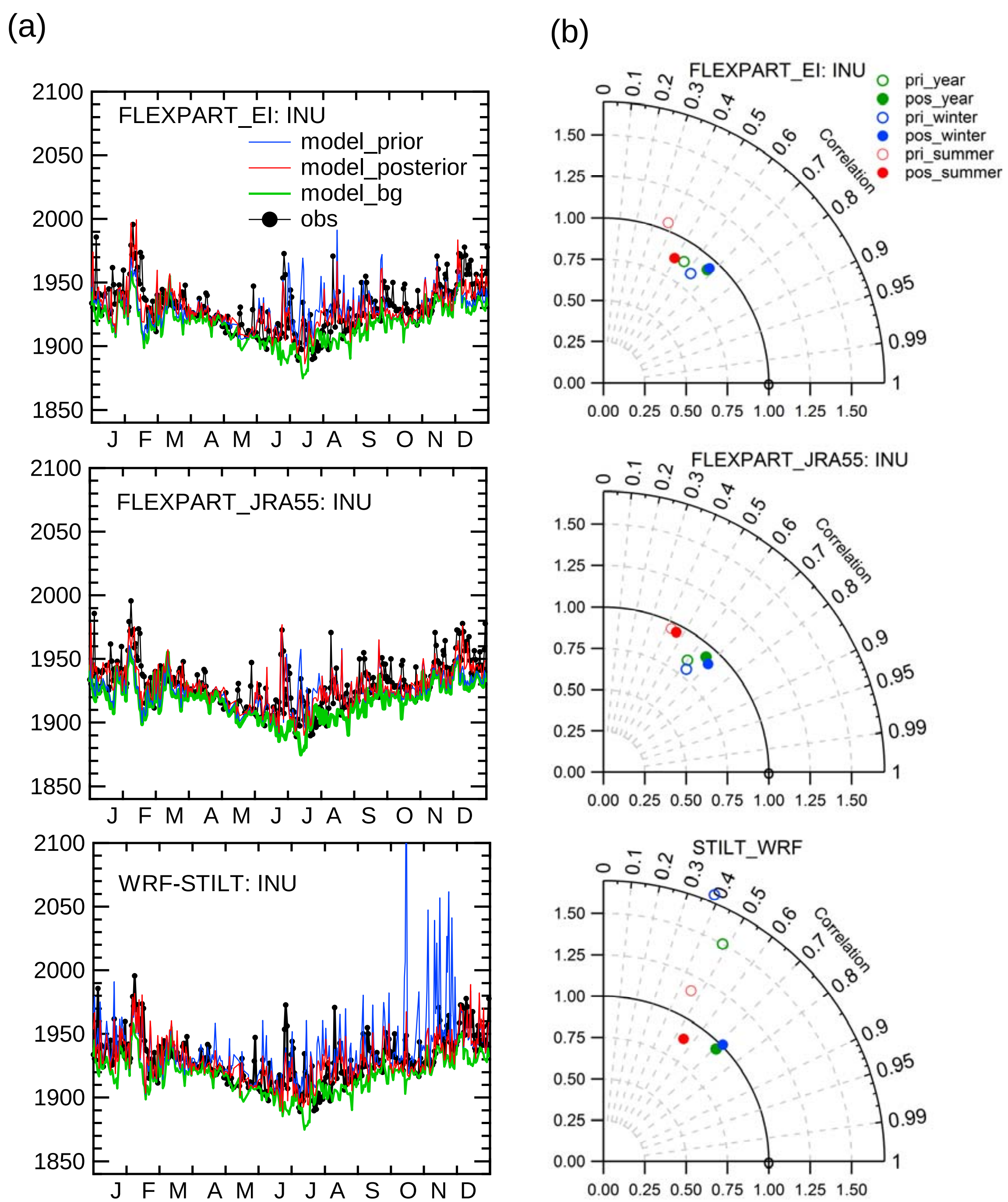

Figure S7: (a) Simulated concentrations for Inuvik with prior and posterior fluxes by three different transport models for 2015, with inversion set up of Mask B and prior flux case C3. The modelled background concentrations and observations are also plotted. (b) Taylor diagrams for comparison between prior and posterior concentrations. The correlation coefficients and normalised standard divinations (NSD) are calculated for summer (June–September), winter (October–May) and throughout years for 2012─2015.

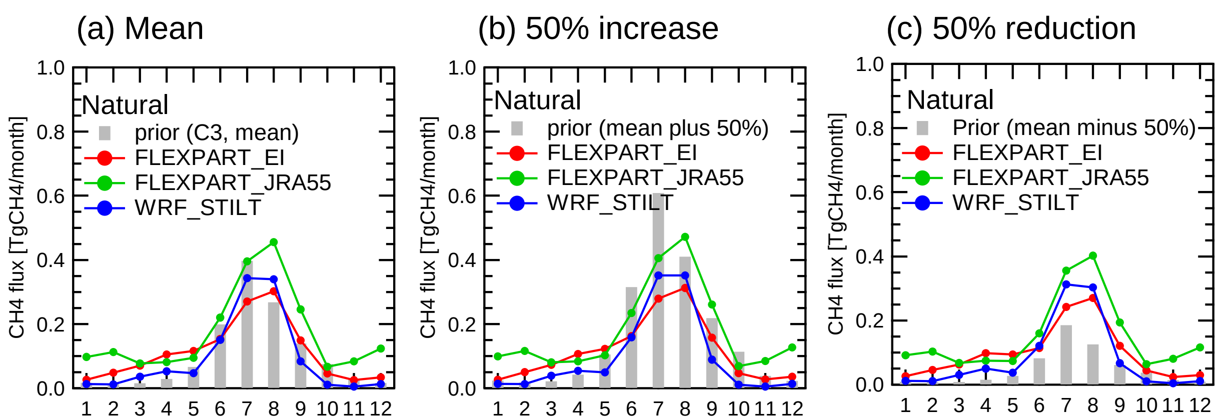

Figure S8: Four-year (2012─2015) mean optimised natural CH_4 fluxes for the entire Canadian Arctic, with prior flux case C3, but three different prior wetland fluxes, (a) WetCHARTs mean (same as C3), (b) WetCHARTs mean with 50% increase, and (c) WetCHARTs mean with 50 % reduction.

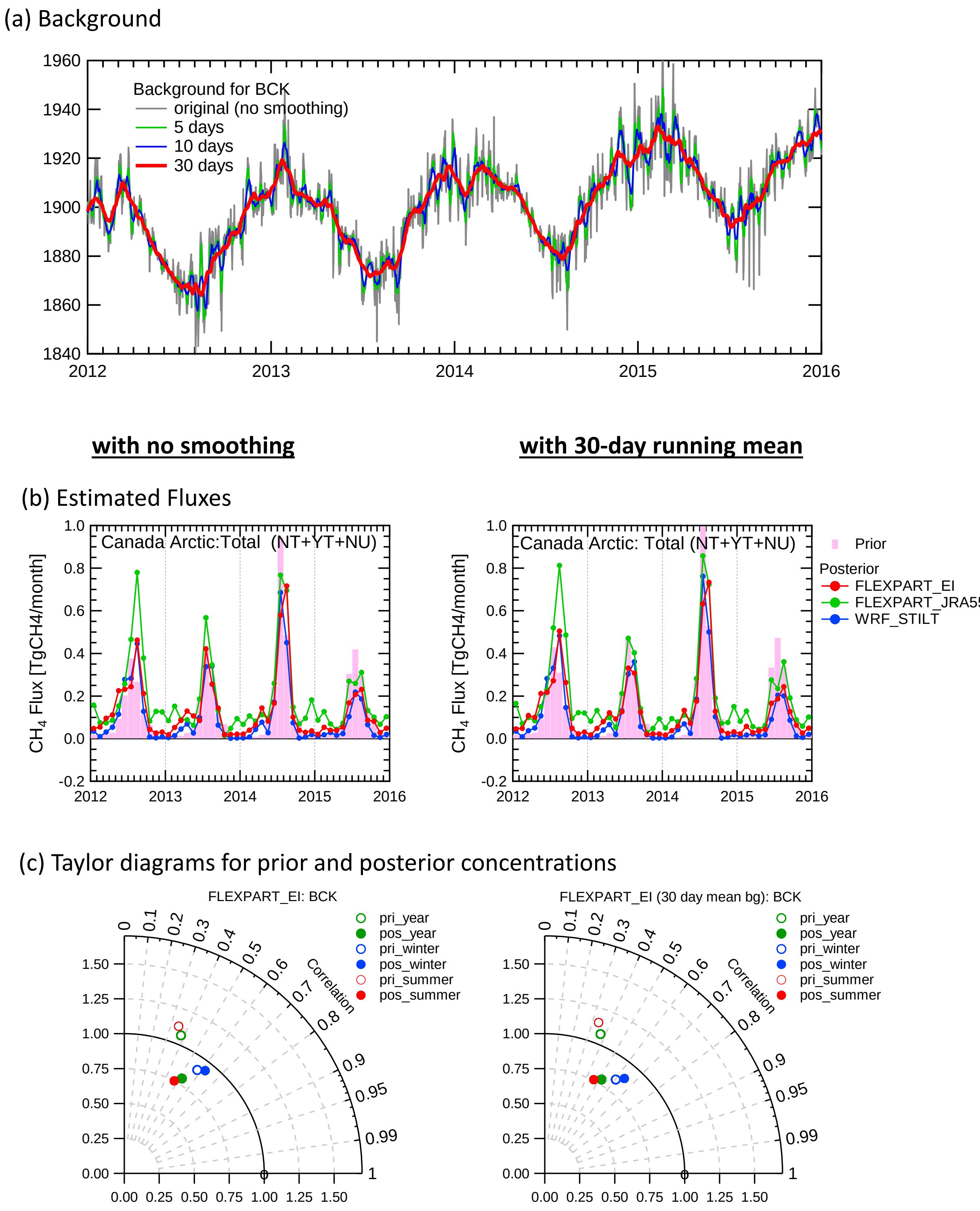

Figure S9: Impact of background concentrations. (a) the background concentrations for Behchoko (BCK) with no smoothing (black), 5-day (green), 10-day (blue) and 30-day (red) running mean. (b) Estimated total fluxes for the entire Canadian Arctic with background with no smoothing (left) and with 30-day running mean (right) in the experiments with Mask B and Prior emission C3 by FLEXPART_EI (red), FLEXPART_JRA55 (green) and WRF-STILT (blue). The prior fluxes are indicated by pink histograms. (c) Taylor diagram for comparison of prior (open circles) and posterior (closed circles) concentrations by FLEXPART_EI for the entire period and winter/summer seasons between the non-smoothed background (left) and smoothed background (right).